

Angular Tunneling Ionization Probability of Fixed-in-Space H₂ Molecules in Intense Laser Pulses

A. Staudte,¹ S. Patchkovskii,¹ D. Pavičić,¹ H. Akagi,^{1,3} O. Smirnova,¹ D. Zeidler,¹ M. Meckel,^{1,2} D. M. Villeneuve,¹
R. Dörner,² M. Yu. Ivanov,¹ and P. B. Corkum¹

¹National Research Council, 100 Sussex Drive, Ottawa, Ontario, Canada K1A 0R6

²Institut für Kernphysik, Universität Frankfurt, D-60486 Frankfurt, Germany

³Quantum Beam Science Directorate, Japan Atomic Energy Agency, Tokai-mura, Naka-gun, Ibaraki 319-1195, Japan

(Received 5 October 2008; published 23 January 2009)

We propose a new approach to obtain molecular frame photoelectron angular distributions from molecules ionized by intense laser pulses. With our method we study the angular tunnel ionization probability of H₂ at a wavelength of 800 nm over an intensity range of $2\text{--}4.5 \times 10^{14}$ W/cm². We find an anisotropy that is stronger than predicted by any existing model. To explain the observed anisotropy and its strong intensity dependence we develop an analytical model in the framework of the strong-field approximation. It expresses molecular ionization as a product of atomic ionization rate and a Fourier transform of the highest occupied molecular orbital filtered by the strong-field ionization process.

DOI: 10.1103/PhysRevLett.102.033004

PACS numbers: 33.80.Rv, 31.90.+s, 32.80.Fb, 32.80.Rm

Molecular frame photoelectron angular distributions (MFPADs) provide a powerful tool to study molecular structure. Photoelectrons produced by x-ray or vacuum ultraviolet photons, from a synchrotron (e.g., [1]) or a frequency upconverted laser (e.g., [2]), can illuminate molecules from “within” [3]. There, a single photon ionizes an electron from a core orbital leaving the molecule in a highly excited state that decays quickly, typically followed by rapid disassociation of the molecule (e.g., [4]). The molecular fragments are detected in coincidence with the photoelectron to yield MFPADs. In contrast, in the limit of multiphoton or tunneling ionization, characteristic for strong laser fields, the highest occupied molecular orbital (HOMO) is most efficiently ionized, thereby creating ground-state ions that are often stable against dissociation. Hence, the alignment of the molecules [5] prior to ionization has been imperative for gaining access to MFPADs in strong laser fields [6,7]. However, this approach has limitations. First, the achievable degree of alignment is limited, in particular, for weakly anisotropic molecules such as H₂ [8–10]. Second, it is insensitive to the orientation of heteronuclear molecules.

We introduce a new experimental approach to measure molecular frame photoelectron angular distributions in intense laser pulses that does not require active alignment. Similar to single photon studies, we infer the molecular alignment from dissociation fragments after the molecule has been ionized. We present the first experimental results of the angle dependent tunneling ionization rate for H₂.

For theory the calculation of MFPADs presents a major challenge. In the single photon case an extensive literature even for arbitrary alignments is available (e.g., [11,12]). For multiphoton ionization, on the other hand, fully correlated simulations for the simplest multielectron molecule, i.e., H₂, have been performed, but only for a single alignment geometry [13]. For arbitrary alignment, the two-electron simulations of H₂ have so far relied on the time-

dependent Hartree-Fock approximation [14]. Among analytical models, the most successful are the molecular tunneling theory [15] and the molecular strong-field approximation (MOSFA), e.g., [16–18].

We combine the MOSFA approach with the saddle-point analysis of the arising integrals to obtain a simple analytical expression. Our model agrees very well with the intensity dependence of the experiment and predicts an even higher degree of anisotropy than is measured in stark contrast to any other existing model.

The experiment was performed using cold target recoil ion momentum spectroscopy (COLTRIMS) [19] and specific details of our apparatus have been published elsewhere [20]. Circularly polarized Ti:sapphire laser pulses (40 fs, 800 nm) are focused to peak intensities of $2.0\text{--}4.5 \times 10^{14}$ W/cm² into a gas jet from a supersonic expansion of natural H₂, at a stagnation pressure of 2 bar through a nozzle with a diameter of 6 μm that was precooled to 50 K preparing the molecules in the rovibrational ground state [21].

Figure 1(a) highlights the two critical parts of our experiment. In the first step ground state H₂ molecules ($X^1\Sigma_g^+(v=0, j=0)$) are singly ionized by a circularly polarized laser pulse. The liberated electron drifts away from its parent ion as determined by the laser field. Simultaneously, the laser field couples the $1s\sigma_g$ ground state of the H₂⁺ with its first excited state, the $2p\sigma_u$, resulting in the dissociation of H₂⁺ into a proton and a hydrogen atom. Since the dissociation occurs during the femtosecond laser pulse the axial recoil approximation [22] necessary for fixed-in-space molecules is valid.

This rapid dissociation is called bond softening and has been extensively discussed, e.g., in Refs. [23,24]. In general, it refers to the mechanism by which a bound state is coupled to a dissociative state through the laser field. Figure 1(b) illustrates this for H₂⁺. Tunneling ionization of H₂ creates a vibrational wave packet on the $1s\sigma_g$ surface

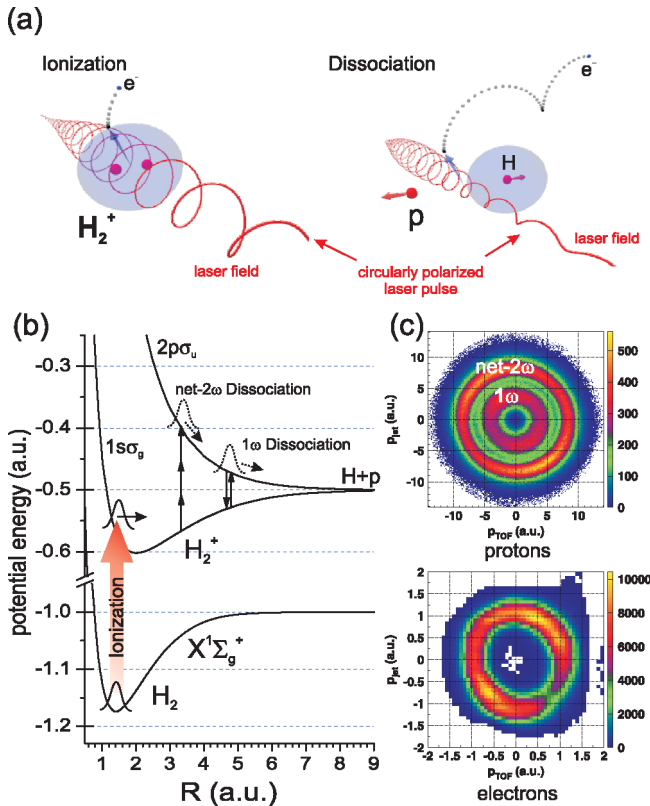


FIG. 1 (color online). (a) Sketch of the experiment. The same circularly polarized laser pulse ionizes (left) and subsequently dissociates (right) the molecule. (b) Potential energy curves of H_2 and H_2^+ indicating the pathways leading to 1 photon and net-2 photon dissociation of H_2^+ . (c) Top: Measured proton momentum distribution produced by dissociating H_2^+ in the polarization plane of a circularly polarized, 800 nm, 40 fs pulse at 3.0×10^{14} W/cm². Bottom: electron momentum distribution produced by single ionization of H_2 under identical conditions.

of H_2^+ . Absorption of an odd number of photons allows the molecule to transfer to the $2p\sigma_u$ state resulting in discrete dissociation velocities according to the number of absorbed photons. In the case of 3 photon absorption the wave packet will transfer back to the $1s\sigma_g$ at the 1 photon resonance by stimulated emission of a photon. Hence, this channel is called net-2 photon dissociation. In circular laser fields bond softening can proceed in any direction within the polarization plane giving rise to a donut shaped momentum space of dissociation fragments as shown in the upper panel of Fig. 1(c). The internuclear axis is confined within the polarization plane to $\pm 15^\circ$ and $\pm 6^\circ$ for the 1 photon and net-2 photon channel, respectively.

Now we turn to the ionization step preceding bond softening. For circular polarization (i.e., ellipticity $\epsilon = 1$), the observable electron momentum is proportional in magnitude and, within the polarization plane, perpendicular in direction to the field at the instant of tunneling [25,26]. Hence, a circularly polarized laser pulse yields a donut shaped electron momentum distribution [lower panel in Fig. 1(c)]. An ellipticity close to unity incurs a mapping

error that does not exceed $\delta\vartheta = \delta E/E$. Even for ultrashort (< 6 fs), large bandwidth pulses it is possible to achieve $\epsilon \approx 95\%$, i.e., $\delta\vartheta \leq 18^\circ$ [26]. Another uncertainty in the electron direction arises from the spread of the initial momentum at the time of tunneling which can be estimated from the perpendicular component p_\perp of its final drift momentum p_f . Examining the electron emission angle out of the polarization plane we find an angular uncertainty of $\pm 13^\circ$ (FWHM) at 2×10^{14} W/cm², which is expected to increase with intensity.

Figure 2(a) shows a polar plot of the MFPAD of H_2 , i.e., the angular ionization probability of the HOMO. The peak intensity was 2.3×10^{14} W/cm² and only molecules dissociated via the net-2 photon channel were considered. The experimental data points $w(\theta)$ are fitted to $\sqrt{w_\perp \sin^2\theta + w_\parallel \cos^2\theta}$ (solid line). The ratio of the ionization yields w_\parallel/w_\perp , provided in the figure, is used to parametrize the observed anisotropy in the ionization probability.

Molecules lying out of the plane of polarization will also be ionized. However, those molecules cannot dissociate via bond softening. Yet, the laser induced prompt alignment [27] into the plane of polarization within the duration of the laser pulse will allow some of those out-of-plane molecular ions to bond soften. This leads eventually to a small systematic underestimation for the ionization asymmetry.

Figure 2(b) plots the intensity dependence of this ratio w_\parallel/w_\perp . We have analyzed the angular distributions for each of the bond softening channels separately (circles—1 photon; triangles—net-2 photon) and also combined (squares). The latter reflects the intensity dependence of the relative strength of both channels. At all intensities hydrogen ionizes preferentially along the molecular axis with the anisotropy decreasing for higher intensities. In contrast to the experiment, the molecular tunneling model of Ref. [28] (dashed line) does not predict any measurable intensity dependence. Numerical simulations of the time-

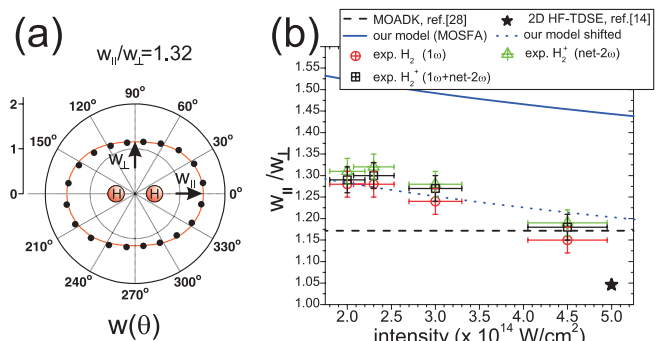


FIG. 2 (color online). (a) MFPAD of H_2 ($X^1\Sigma_g^+$) in circularly polarized, 40 fs, 800 nm laser pulses at 2.3×10^{14} W/cm². (b) Ratio of the ionization rates w_\parallel/w_\perp as a function of intensity for experiment and theory. Dashed line: MOADK [28], solid star: Hartree-Fock calculation [14]. Solid line: our model—length-gauge MOSFA (see text for details).

dependent Schrödinger equation in Hartree-Fock approximation [14] (star), with electron motion restricted to two dimensions, suggests a far more symmetric ionization probability than experiment shows.

While the experimental peak intensities cover a range of the Keldysh adiabaticity parameter γ [29] of 1.1 to 0.8, it has been demonstrated that tunneling is a valid description of the ionization process for γ at least up to 1.45 [26]. Particularly it was shown in Ref. [18], that length-gauge MOSFA not only reproduces the correct qualitative angular distribution but also provides very good agreement in the overall ionization rate for γ as high as 1.6. Hence, to describe the observed anisotropy in the ionization probability, we have developed a simple model based on the length-gauge MOSFA.

In the derivation, we deal with the potential artifacts arising when applying length-gauge strong-field approximation (SFA) to molecules [30]. Polarization and associated Stark shift of the two-electron ground state are calculated *ab initio*, for a constant electric field, using the configuration interaction (CI) method.

We begin by writing the continuum wave function of the liberated electron in the momentum space, in the length gauge

$$\Psi(\mathbf{p}, t) = -i \int_{t_0}^t dt' e^{-iS(\mathbf{p}, t, t')} \mathbf{E}(t') \langle \mathbf{p}(t') | \hat{\mathbf{r}} | \Phi_g \rangle. \quad (1)$$

Here $|\Phi_g\rangle$ is the ground state, \mathbf{p} is the instantaneous kinetic momentum of the electron, $\mathbf{p}(t') = \mathbf{p} + \mathbf{A}(t') - \mathbf{A}(t)$, $\mathbf{A}(t)$ is the laser vector-potential, and \mathbf{E} is the electric field. The phase S contains the Volkov phase, the contribution of the field-free ionization potential I_p , and the difference $\Delta(\tau)$ between the quasistatic Stark shifts of the neutral and the ion:

$$S(\mathbf{p}, t, t') = \int_{t'}^t d\tau \frac{|\mathbf{p} - \mathbf{A}(t) + \mathbf{A}(\tau)|^2}{2} - \int_{t_0}^{t'} d\tau [I_p + \Delta(\tau)]. \quad (2)$$

The quasistatic Stark shifts are included in $I_p(\tau)$. The molecular specifics enters via $|\Phi_g\rangle$, approximated by the highest occupied molecular orbital (HOMO). We write it as a linear combination of identical atomic orbitals $\Phi_g(\mathbf{r}) = \sum_i C_i \phi_a(\mathbf{r} - \mathbf{r}_i)$, which can always be done (e.g., Gaussian basis). The coefficients C_i can depend on the external field, reflecting polarization of the ground state.

Substituting this expression into Eq. (1) and following [30], we remove the terms proportional to $\langle \mathbf{p}' | \phi_a \rangle$ that arise due to nonorthogonality of the continuum to the bound states in the SFA. The result is

$$\Psi(\mathbf{p}, t) = -i \sum_i C_i \int_{t_0}^t dt' e^{-iS(\mathbf{p}, t, t')} \mathbf{E}(t') \mathbf{d}[\mathbf{p}(t')] e^{-i\mathbf{p}(t') \cdot \mathbf{r}_i} \quad (3)$$

where $\mathbf{d}[\mathbf{p}] = \langle \mathbf{p} | \hat{\mathbf{r}} | \phi_a \rangle$ is the transition dipole for an orbital centered at the origin. The difference from the case of a

single atomic orbital is the presence of the $\sum_i C_i$, with phase factors $e^{-i\mathbf{p}(t') \cdot \mathbf{r}_i}$.

To proceed further, we assume linear polarization. Comparing with experiment, we take the same field strength as for the circularly polarized field. Following Ref. [31], we begin by setting $\mathbf{p}(t) = 0$ and look for the closest to t saddle point of the t' integral. For each atomic orbital, the saddle-point condition is $\mathbf{p}_{\parallel}^2(t')/2 + I_{p,i}(t') = 0$, with $I_{p,i}(t') = I_p + \Delta(t') + \mathbf{E}_L(t') \cdot \mathbf{r}_i$ including the voltage $\mathbf{E}_L(t') \cdot \mathbf{r}_i$ at the position of the orbital. As discussed in [30], when the electron density is strongly polarized and the Stark shift approaches linear regime, this voltage is canceled. In that regime, typical for larger molecules, it is crucial to include field dependence of C_i . Here, the Stark shift remains approximately quadratic, the voltages are small compared to I_p , and $p_{\parallel}(t') \approx -i\kappa = -i\sqrt{2I_p}$ is time independent. From Eq. (3) we see that this adds time-independent factors $\exp(-\kappa r_{i,\parallel})$ at the saddle point. For nonzero transverse momenta $p_{\perp} \neq 0$, the phase $\exp(-ip_{\perp} r_{i,\perp})$ is also time independent and is taken out of the integral in Eq. (3). The result is

$$\begin{aligned} \Psi(p_{\perp}, t) &\approx \Psi_a(p_{\perp}, t) \sum_i C_i e^{-\kappa r_{i,\parallel}} e^{-ip_{\perp} r_{i,\perp}} \Psi_a(p_{\perp}, t) \\ &= -i \int_{t_0}^t dt' e^{-iS(\mathbf{p}, t, t')} \mathbf{E}(t') \mathbf{d}[\mathbf{p}(t')]. \end{aligned} \quad (4)$$

Up to a preexponential factor, the subcycle ionization rate is proportional to $\int dp_{\perp} |\Psi(p_{\perp}, t)|^2$ [32]. We now recall that $\Psi_a(p_{\perp}, t) \propto \Psi_a(0, t) \exp(-p_{\perp}^2 \tau_T/2)$ (see, e.g., [33]), where τ_T is the tunneling time given by $E/\omega \sinh \omega \tau_T = \kappa$. That is, tunneling introduces a filter for the initial transverse distribution. Integrating over transverse momentum distribution yields the rate

$$\Gamma(\theta, t) = \Gamma_0(\theta, t) F(\theta), \quad (5)$$

$$F(\theta) \approx \frac{\int dp_{\perp} e^{-p_{\perp}^2 \tau_T} |\sum_i C_i e^{-ip_{\perp} r_{i,\perp}} e^{-\kappa r_{i,\parallel}}|^2}{\int dp_{\perp} e^{-p_{\perp}^2 \tau_T}}, \quad (6)$$

where $\Gamma_0(\theta, t)$ is the rate for a ‘‘single’’ atomic orbital, and $F(\theta)$ is the molecular interference term, normalized to a single atomic orbital. The rate $\Gamma_0(\theta)$ depends on the molecular orientation via the θ -dependent Stark shift. It incorporates Coulomb correction factors to ensure correct asymptotic dependence in the quasistatic tunneling limit. Depending on the problem, one can use either cycle-averaged expressions derived by Popov and coworkers [34] or subcycle rates from [32], valid both for small and intermediate values of the Keldysh parameter γ .

For the hydrogen molecule, we approximate the ground state HOMO as a sum of two atomic orbitals centered at $r_i = \pm R/2$, with $C_1 = C_2 = 1/\sqrt{2Z}$, where $Z = 1 + \langle \phi_a(\mathbf{r} - \mathbf{R}/2) | \phi_a(\mathbf{r} + \mathbf{R}/2) \rangle$. Then

$$F(\theta) \approx \frac{e^{\kappa R \cos \theta} + e^{-\kappa R \cos \theta} + 2e^{-(R^2 \sin^2 \theta / 4\tau_T)}}{2Z}, \quad (7)$$

where θ is the angle between molecular axis and laser polarization. The first term comes from the downhill atomic orbital, which is more likely to contribute to ionization. The second term comes from the uphill orbital, and the third is the cross-term due to the interference of the two atomic orbitals in the ionization. The origin of the $\exp(\kappa R)$ term for an extended potential well is the reduction in the height of the barrier by $R/2E$. If the electron were to localize in the downhill well, this reduction would have been exactly compensated for by the linear Stark shift of the ground state. However, this is not the case at the intensities studied here: our calculations show that the Stark shift remains quadratic up to $I = 2 \times 10^{14}$ W/cm² for linear polarization, and hence we use known static polarizabilities.

For comparison with the experiment the anisotropy in ionization probability $\Gamma(0^\circ)/\Gamma(90^\circ)$ is shown as the solid line in Fig. 2(b). For all intensities the model predicts a considerably higher degree of anisotropy than the experiment. However, as discussed above, the experiment underestimates the actual asymmetry. Molecules may lie out of the polarization plane. For these molecules the anisotropy will be reduced from that of the perfectly aligned molecule.

The second prominent feature shared by both the experiment and theory is the intensity dependence of the anisotropy. The ac-Stark shift in $\Gamma_0(\theta)$ is larger along the molecular axis and affects the ion more than the neutral molecule. However, the electron interaction with the induced dipole of the molecular ion compensates the ac-Stark shift in the molecular ion completely [35]. This leads to the counterintuitive result of an increased ionization potential along the molecular axis. However, the shape of the molecular orbital, included through the molecular interference term $F(\theta)$, overcompensates the Stark shift and is responsible for the observed anisotropy. With increasing intensity the Stark shift diminishes the anisotropy in the ionization probability.

In conclusion, we have introduced a new method for measuring the angle dependent ionization probability. Based on correlation, we estimate a measurement accuracy of $\pm 15^\circ$. Furthermore, the method can be applied to heteronuclear molecules.

To our knowledge, ours is the first measurement of the angle dependent ionization probability for molecular hydrogen. It has been argued that this information is of vast importance in disentangling recollision cross sections [18]. From other studies on H₂ it is known [36] that the differential cross section for recollision excitation changes by an order of magnitude between parallel and perpendicular alignment. Our experiment shows that at least 30% of the effect is caused by the angle dependence of the tunneling probability.

Turning to theory, our intuition of tunneling is that the electron escapes from those regions of the wave function

that are nearest to the suppressed potential. By using the length gauge, the spatial character of tunneling is included.

We are indebted to S. Montero for helpful discussions. The experimental work is supported by an NSERC accelerator grant, AFOSR, NSERC Centre-of-Excellence for Photonic Innovation, NRC HGF science and technology fund, Deutsche Forschungsgemeinschaft, Alexander-von-Humboldt Stiftung, and the Studienstiftung des deutschen Volkes.

Note added in proof.—Recently, we became aware of a similar experiment and encompassing *ab initio* calculations performed deep in the tunneling regime by using a longer wavelength [37].

-
- [1] E. Shigemasa *et al.*, Phys. Rev. Lett. **74**, 359 (1995).
 - [2] O. Geßner *et al.*, Science **311**, 219 (2006).
 - [3] A. Landers *et al.*, Phys. Rev. Lett. **87**, 013002 (2001).
 - [4] K. Kreidi *et al.*, Phys. Rev. Lett. **100**, 133005 (2008).
 - [5] H. Stapelfeldt and T. Seideman, Rev. Mod. Phys. **75**, 543 (2003).
 - [6] I. V. Litvinyuk *et al.*, Phys. Rev. Lett. **94**, 033003 (2005).
 - [7] D. Pavičić *et al.*, Phys. Rev. Lett. **98**, 243001 (2007).
 - [8] K. F. Lee *et al.*, J. Phys. B **39**, 4081 (2006).
 - [9] W. A. Bryan *et al.*, Phys. Rev. A **76**, 023414 (2007).
 - [10] I. A. Bocharova *et al.*, Phys. Rev. A **77**, 053407 (2008).
 - [11] W. Vanroose *et al.*, Phys. Rev. A **74**, 052702 (2006).
 - [12] J. Colgan *et al.*, Phys. Rev. Lett. **98**, 153001 (2007).
 - [13] M. Awasthi and A. Saenz, J. Phys. B **39**, S389 (2006).
 - [14] N. Hay *et al.*, J. Mod. Opt. **50**, 561 (2003).
 - [15] X. M. Tong *et al.*, Phys. Rev. A **66**, 033402 (2002).
 - [16] J. Muth-Böhm *et al.*, Phys. Rev. Lett. **85**, 2280 (2000).
 - [17] A. Becker and F. H. M. Faisal, J. Phys. B **38**, R1 (2005).
 - [18] T. K. Kjeldsen and L. B. Madsen, J. Phys. B **37**, 2033 (2004).
 - [19] J. Ullrich *et al.*, Rep. Prog. Phys. **66**, 1463 (2003).
 - [20] A. Staudte *et al.*, Phys. Rev. Lett. **98**, 073003 (2007).
 - [21] S. Montero *et al.*, J. Chem. Phys. **125**, 124301 (2006).
 - [22] R. N. Zare, J. Chem. Phys. **47**, 204 (1967).
 - [23] A. Zavriyev *et al.*, Phys. Rev. A **42**, 5500 (1990).
 - [24] A. Giusti-Suzor *et al.*, Phys. Rev. Lett. **64**, 515 (1990).
 - [25] P. B. Corkum *et al.*, Phys. Rev. Lett. **62**, 1259 (1989).
 - [26] P. Eckle *et al.*, Science **322**, 1525 (2008).
 - [27] P. W. Dooley *et al.*, Phys. Rev. A **68**, 023406 (2003).
 - [28] X. M. Tong *et al.*, Phys. Rev. A **68**, 043412 (2003).
 - [29] L. V. Keldysh, Sov. Phys. JETP **20**, 1307 (1965).
 - [30] O. Smirnova *et al.*, J. Mod. Opt. **54**, 1019 (2007).
 - [31] G. L. Yudin and M. Yu. Ivanov, Phys. Rev. A **63**, 033404 (2001).
 - [32] G. L. Yudin and M. Yu. Ivanov, Phys. Rev. A **64**, 013409 (2001).
 - [33] M. Yu. Ivanov *et al.*, J. Mod. Opt. **52**, 165 (2005).
 - [34] V. S. Popov, Phys. Usp. **47**, 855 (2004).
 - [35] P. Dietrich and P. B. Corkum, J. Chem. Phys. **97**, 3187 (1992).
 - [36] H. Niikura *et al.*, Nature (London) **417**, 917 (2002).
 - [37] I. V. Litvinyuk *et al.* (private communication).